Numerical analysis of a viscous steady laminar flow due to a mass transfer from a porous plate

Received January 1996
Revised October 1996
Accepted February 1997

André Desseaux
Université de Valenciennes, Laboratoire de Mécanique des Fluides et d'Energétique, Valenciennes, Cedex, France

Introduction

Many carrying or support systems have been used in high-technology industries. In these systems, support or conveyance without contact with supporting devices is a major problem. There are many ideas for the supporting and carrying systems. Two types of supporting systems using air flow have been proposed. One is to remove air from the device and the other is to eject air from small slits or from a uniformly porous surface to generate positive pressure on the surface. In the latter case, within the past few years, many problems have been studied dealing directly with the fluid flow through porous media. Examples of these are the cases of transpiration cooling, boundary-layer control or sustentation.

To simulate conditions encountered in the suspension problem, the configuration investigated here is that of a flow in the gap between an infinite uniformly porous plate and a disk able to move in a direction perpendicular to the porous surface.

With another configuration, Petit (1986) has shown effects of viscosity. The sustentation of an air-cushion pad when air is blown out from an annular ring is studied by Nakajima *et al.* (1995). An experimental investigation for the pressure is presented by Crnojevic *et al.* (1995) if air is ejected through a circular aperture.

The disk floats at the distance $\underline{h}$ above a porous surface. We treat the problem as a steady, incompressible, axially symetrical flow and we limit our study to a Reynolds number greater than 1.

Defining equations of sustentation

The dimensional velocity is expressed in $\underline{r}$ and $\underline{z}$ (here, the underline indicates a dimensional quantity):

$$V = \underline{u}.r + \underline{v}.z \quad (1)$$

The author thanks Professor John A. Reizes, University of New South Wales, Australia, for many long and valuable comments on an earlier draft of the manuscript.

International Journal of Numerical Methods for Heat & Fluid Flow
Vol. 8 No. 2, 1998, pp. 169–182.

and we consider the case of a circular disk of radius $\underline{R}$ and a constant rate at the porous wall in the form:

$$\underline{v}(0) = 2.\underline{q} \tag{2}$$

If $\underline{h}$ is the stabilized dimensional height above the porous surface, the mean peripherical velocity $\underline{U}$ is given by

$$\underline{U}.\underline{h} = \int_0^{\underline{h}} \underline{u}.d\underline{z} = \underline{R}.\underline{q} \tag{3}$$

The conservation equations for this two-dimensional axisymetric flow are

continuity

$$\frac{\partial \underline{u}}{\partial \underline{r}} + \frac{\underline{u}}{\underline{r}} + \frac{\partial \underline{v}}{\partial \underline{z}} = 0 \tag{4}$$

$\underline{r}$-momentum equation

$$\rho.\left(\underline{u}.\frac{\partial \underline{u}}{\partial \underline{r}} + \underline{v}.\frac{\partial \underline{u}}{\partial \underline{z}}\right) = -\frac{\partial \underline{p}}{\partial \underline{r}} + \mu.\left(\frac{\partial^2 \underline{u}}{\partial \underline{r}^2} + \frac{1}{\underline{r}}.\frac{\partial \underline{u}}{\partial \underline{r}} - \frac{\underline{u}}{\underline{r}^2} + \frac{\partial^2 \underline{u}}{\partial \underline{z}^2}\right) \tag{5}$$

$\underline{z}$-momentum equation

$$\rho.\left(\underline{u}.\frac{\partial \underline{v}}{\partial \underline{r}} + \underline{v}.\frac{\partial \underline{v}}{\partial \underline{z}}\right) = -\frac{\partial \underline{p}}{\partial \underline{z}} + \mu.\left(\frac{\partial^2 \underline{v}}{\partial \underline{r}^2} + \frac{1}{\underline{r}}.\frac{\partial \underline{v}}{\partial \underline{r}} + \frac{\partial^2 \underline{v}}{\partial \underline{z}^2}\right) \tag{6}$$

Scaling transformation is one of the most prominent transformations in fluid flow problems. We first scale all the dependent and independent variables as follows.

$$\underline{r} = \underline{R}.r \quad ; \quad \underline{z} = \underline{h}.z \tag{7}$$

and

$$\underline{u} = \underline{U}.u \quad ; \quad \underline{v} = 2.\underline{q}.\vartheta \tag{8}$$

Unfortunately, we do not know which characteristic is able to scale the pressure. Using the rate of blowing, we can write:

$$\underline{p} = p.\left(\rho.\underline{q}^2\right) \tag{9}$$

Using this definition of non-dimensional pressure and equation (3) the $\underline{z}$-momentum equation (6) becomes

$$u.\frac{\partial \vartheta}{\partial r} + 2.\vartheta.\frac{\partial \vartheta}{\partial z} = -\frac{1}{2}.\frac{\partial p}{\partial z} + \frac{\nu}{\underline{h}\underline{q}}.\left[\left(\frac{\underline{h}}{\underline{R}}\right)^2\left\{\frac{\partial^2 \vartheta}{\partial r^2} + \frac{1}{r}\frac{\partial \vartheta}{\partial r}\right\} + \frac{\partial^2 \vartheta}{\partial z^2}\right] \quad (10)$$

In (10), two non-dimensional numbers appear:

(1) the Reynolds number $\underline{h} \cdot \underline{q}/\underline{\nu}$ in which we find the rate of blowing at the porous surface;

(2) a dimensionless characteristic ε defined as the ratio of the height $\underline{h}$ and the radius $\underline{R}$ of the disk. In order for a support system to operate, ε has to be small.

We look for a solution of equation (10) which can eliminate the influence of ε. In this case this means that:

$$\frac{\partial^2 \vartheta}{\partial r^2} + \frac{1}{r}\frac{\partial \vartheta}{\partial r} = 0 \quad (11)$$

which leads to a general solution

$$\vartheta = Z(z).\left(K_1.\mathrm{Log}\, r + K_2\right) \quad (12)$$

A solution must be valid on the axis of symmetry ($r = 0$) and requires that this component of velocity depends only on the variable z ($K_1 = 0$) so that:

$$\vartheta = Z(z) \quad (13)$$

With (13), continuity equation is reduced to:

$$\frac{\partial u}{\partial r} + \frac{u}{r} = -2.\frac{dZ}{dz} \quad (14)$$

and a solution for the radial component of the velocity which can verify the condition on the axis of symmetry and the boundary conditions is

$$u = -r.\frac{dZ}{dz} \quad (15)$$

We have found with (13) and (15) that the two velocity components are expressed in the form of a unique complementary function. This solution is equivalent to a self-similar solution.

On the other hand, we can use the mean radial velocity $\underline{U}$ to scale the pressure

$$\underline{p} = p.\left(\rho\,\underline{U}^2\right) \quad (16)$$

Introducing (13), (15) and (16) in the two momentum equations (5) and (10), the next equations appear as

$$Z'^{2} - 2.Z.Z'' + \frac{\nu}{\underline{h}.\underline{q}}.Z''' = -\frac{1}{r}.\frac{\partial p}{\partial r} \tag{17}$$

$$2.Z.Z' - \frac{\nu}{\underline{h}.\underline{q}}.Z'' = -\frac{1}{2}.\left(\frac{\underline{U}}{\underline{q}}\right)^{2}\frac{\partial p}{\partial z} \tag{18}$$

where a differentiation with respect to z of equation (17) and with respect to r of equation (18) leads to the conclusion that the right hand side of equation (17) is independent from the variable. Then, the term depending on the pressure on the right hand side of (17) is a constant α. The value of this constant is given by the value of the third derivative Z''' on the disk:

$$\alpha = \frac{\nu}{\underline{h}.\underline{q}}.Z'''\Big|_{z=1.} \tag{19}$$

We can now express the pressure in dimensional variables as:

$$\underline{p} - \underline{p}^{*} = 2.\rho.\underline{q}^{2}.\left[-\frac{\alpha}{4}.\left(\frac{\underline{r}}{\underline{h}}\right)^{2} - Z^{2} + \frac{\nu}{\underline{h}.\underline{q}}.\left(\frac{dZ}{dz}\right)\right] \tag{20}$$

in which $\underline{p}^{*}$ is a judicious constant of integration.

α can be eliminated by a differentiation of (17) with respect to z and the problem of levitation of a disk is translated into

$$\frac{d^{4}Z}{dz^{4}} = 2.\frac{\underline{h}.\underline{q}}{\nu}.Z.\frac{d^{3}Z}{dz^{3}} = Re.Z.\frac{d^{3}Z}{dz^{3}} \tag{21}$$

with two conditions on the porous surface, namely

$$Z(0) = 1 \quad ; \quad Z'(0) = 0 \tag{22}$$

On the upper side of the domain, the no-slip conditions give

$$Z(1.) = 0 \quad ; \quad Z'(1.) = 0 \tag{23}$$

Quasilinearization method

The method used to find a solution of the non-linear differential equation (21) is the "quasilinearization method" proposed by Radbill (1964). The method is viewed as an extension of the Newton-Raphson method.

Linearization

Following Radbill (1964), equation (21) may be transformed into a linear equation. With the notation

$$f_n = \frac{d^{n-1}Z}{dz^{n-1}} (1 \leq n \leq 4)$$

and two successive solutions $f_n^{(k)}$ and $f_n^{(k+1)}$, a Newton's development of (21) around the previous solution gives

$$\frac{df_4^{(k+1)}}{dz} = Re.\left(f_1^{(k+1)}.f_4^{(k)} + f_4^{(k+1)}.f_1^{(k)} - f_1^{(k)}.f_4^{(k)} \right) \quad (24)$$

Integration scheme

Equation (24) is linear. Replacing the derivatives with five-points central differences approximations:

$$Z''' = \frac{1}{2.h^3}.\left(-\zeta_{k-2} + 2.\zeta_{k-1} - 2.\zeta_{k+1} + \zeta_{k+2} \right) \quad (25)$$

$$Z'''' = \frac{1}{h^4}.\left(\zeta_{k-2} - 4.\zeta_{k-1} + 6.\zeta_k - 4.\zeta_{k+1} + \zeta_{k+2} \right) \quad (26)$$

After eliminating the points ζ_{-1}, ζ_0, ζ_{N+1} and ζ_{N+2} with the boundary conditions and using the approximation

$$Z' = \frac{1}{12.h}.\left(\zeta_{k-2} - 8.\zeta_{k-1} + 8.\zeta_{k+1} - \zeta_{k+2} \right) \quad (27)$$

we get a pentadiagonal matrix for which the easiest method of inversion is the Thomas' algorithm (Salvadori and Baron, 1961). A Richardson extrapolation has been used to improve the accuracy of the calculation.

"TRIO"

The CEA is continually involved in the design fluid flow problems involving heat and mass transfers (Gauvain; Magnaud *et al.*, 1987). With the aim of solving such problems, a family of computer programs has been under development. TRIO is the newest one in the suite of programs called CASTEM 2000. It has been used for many industrial problems as we can see in Gauvain.

TRIO was used to validate the present numerical solution found with the quasilinearization scheme. A moderately fine mesh of 39×26 rectangular elements was used for all the simulations. The grid was made fine close to axis of symmetry and to the disk, coarser near the porous wall and greater and greater with the distance r.

Asymptotic expansion

For low Reynolds, following an idea of Hinch (Hinch and Lemaitre, 1994), we propose the asymptotic polynomial formulation useful for initialization of our scheme.

$$Z \approx \psi_0 + Re.\ \psi_1 \tag{28}$$

with

$$\psi_0 = 1 - 3z^2 + 2z^3 \tag{29}$$

and

$$\psi_1 = \frac{1}{35}\left(22z^2 - 52z^3 + 35z^4 - 7z^6 + 2z^7\right) \tag{30}$$

With (28), we can evaluate the reduced wall shear stress on the disk with

$$Z''(1.) \approx 6. + \frac{26.\,Re}{35} \tag{31}$$

Results and discussion

Convergence

Figure 1 represents a typical case of our calculation. We have used the function Ψ_0 only (29) to initiate the calculation so as to demonstrate the rate of convergence of our scheme in the case of *Re* = 100. The second iteration is very close to the final solution. Typically seven iterations are necessary to reach convergence for each run performed, starting from initial conditions. This number is reduced if the computation is started from the stored solution of a parametrically related previous solution. The convergence of a run is tested on the next quantity (*N* represents the number of the points of the mesh) which must be less than 10^{-6}.

$$\overline{\varepsilon_n(f)} = \sum_{j=1}^{N} \left\{ \left| f_n^{(k+1)}(\zeta_j) \right| - \left| f_n^{(k)}(\zeta_j) \right| \right\} \Big/ N \tag{32}$$

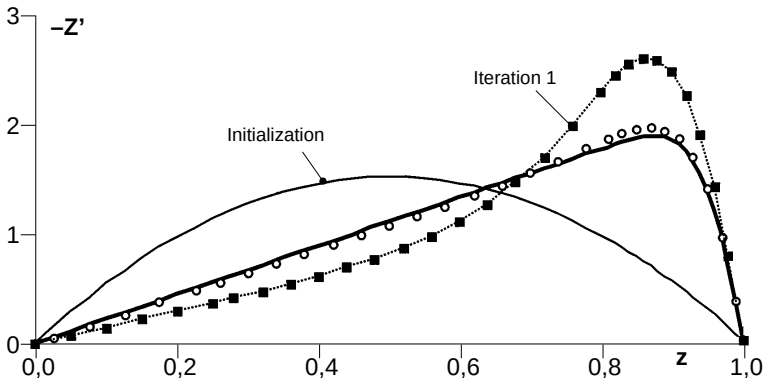

Figure 1.
Convergence for Z' for *Re* = 100 – white dots represent the second iteration and the full line the final solution

Characteristics of the flow

No particular convergence problems were encountered and the residual errors diminished monotically in all the cases presented here. Figures 2-5 represent the conditions on the others boundaries up to $Re = 100$.

An internal procedure of derivation is used in TRIO to obtain Z"(1). It should be remembered that this parameter Z"(1) describes the dimensionless wall shear stress on the disk. The differences between TRIO (except on borders between sub-domains of the mesh) and quasililinearization are negligible.

The two Figures 4 and 5 represent the third derivative of Z. This parameter describes the pressure parameter α (19). We observe that Z"'(0) is rapidly equal

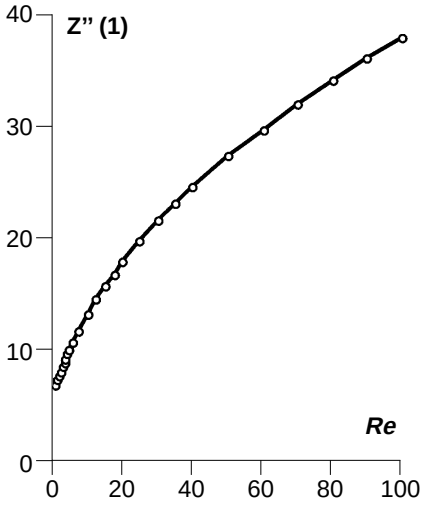

Figure 2.
Second derivative of Z on the disk

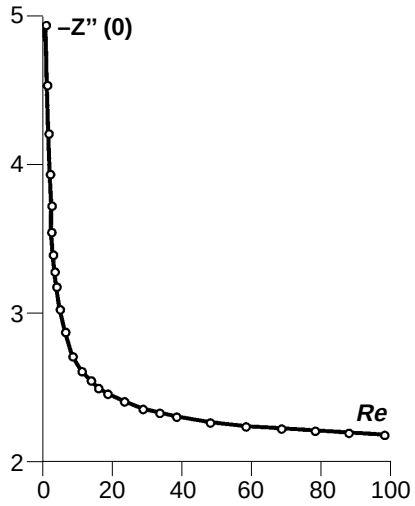

Figure 3.
Second derivative of Z on the porous plate

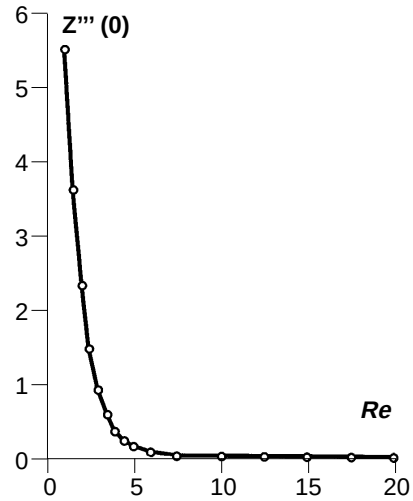

Figure 4.
The third derivative of Z on the porous wall

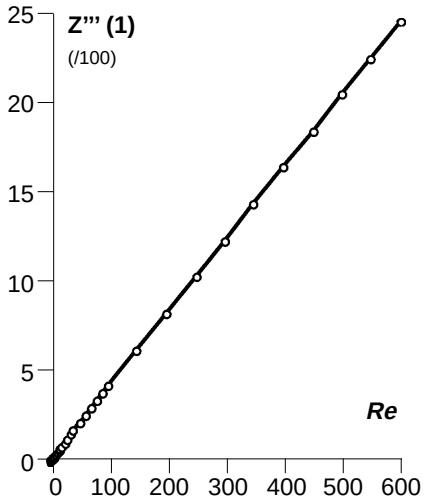

Figure 5.
The third derivative of Z on the disk

to 0. This parameter may be calculated in two manners using equation (17) and the two sets of conditions (22) or (23):

$$\alpha = \left.\frac{\nu}{\underline{h}.\underline{q}}.Z'''\right|_{z=1.} = -2.Z'' + \left.\frac{\nu}{\underline{h}.\underline{q}}.Z'''\right|_{z=0} \tag{33}$$

The difference between the two formulations of α is negligible. For example, for Re = 50, we obtain 4.5164 (z = 0) and 4.5226 on the disk. At Re = 500, this relative difference is less than 0.3 per cent. Using equation (17), we can verify that the non-dimensional pressure gradient is nearly constant all over the domain.

Figure 6 compares Z and Z' (the non dimensional velocity components u and v) for $Re = 2$.

We note that the horizontal component has a nearly parabolic profile and that we cannot see any difference between our results and the approximation given by equation (29). So we have demonstrated that (28) is a useful tool for the initialization of our numerical scheme.

In Figure 7, in which α is plotted against the radius, TRIO gives some inaccurate results at points located at abscissa 1, 2, 4, 8 owing to the step changes in mesh size of our mesh. Near the axis of symmetry, for $r \leq 1$, the pressure parameter given by TRIO (the pressure is recovered from the Navier-Stokes equations with the velocity and, next, derivated) is not constant and differs significantly from our result. The reasons for these differences are:

- the pressure in one element is recovered from the Navier-Stokes equations with the node values of the velocity;
- the node values of the pressure are extrapolated from the value in an element and, thereafter, derived;
- we cannot stipulate all the conditions on the axis of symmetry; we have used only a Dirichlet condition on this frontier.

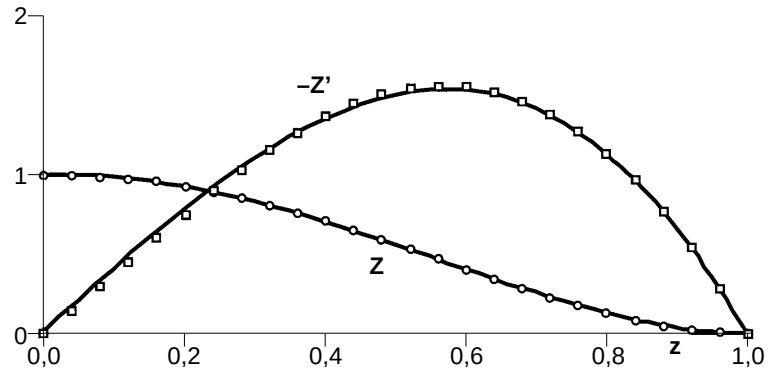

Figure 6. Profiles of the components of velocity – comparison between our numerical results and formula (29) – $Re = 2$

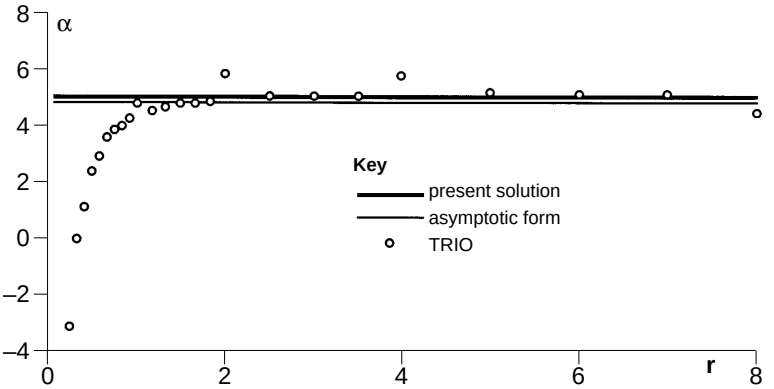

Figure 7. Comparison between our numerical results and TRIO for the pressure parameter α – $Re = 50$

In Figure 7, we can compare our constant numerical value and a second value deduced from (34). This asymptotic expression gives a value lower than our numerical value. The reason for this difference proceeds from the method giving the asymptotic solution. The parameters in (34) are the consequence of a numerical estimation of a displacement thickness. In case of an internal flow, the method generates a loss in the determination of α and the reduced wall shear stress.

The same remarks concerning results obtained with TRIO are also valid for Figure 8 which represents the reduced wall shear stress on the disk for several values of *Re* (1, 5, 15, 25).

Comparison with Hinch's results

We can find in Hinch and Lemaitre (1994), two asymptotic solutions: one for low and the other for high Reynolds numbers supported by some experimental results. Table I compares the reduced wall shear stress on the disk obtained from the asymptotic expansion of *Re* (valid for *Re* > 10)

$$Z''(1.) \approx 3,711\sqrt{Re} \tag{34}$$

with our numerical results.

We see an excellent agreement for low Reynolds numbers and our numerical results are always greater than those obtained with equation (33) for high Reynolds numbers. This remark is also valid in Hinch and Lemaitre (1994) where we can read that "… the high Reynolds number solution is not so accurate until quite large values of the Reynolds number". The reason for this difference is seen in Hinch and Lemaitre (1994) where the final solution is found

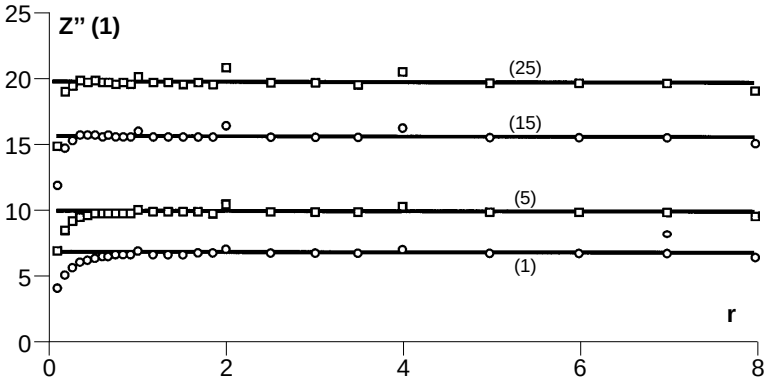

Figure 8.
Comparison between our numerical results and TRIO for the dimensionless wall shear stress on the disk for different values of *Re*

Table I.
The reduced wall shear stress Z"(1), comparison between the present results and asymptotic formulae

Re	Equation (31)	1.0	5.0	Equation (33)	15.00	25.0	50.0
Hinch		6.743	9.715		14.373	18.555	26.241
Present solution		6.768	9.875		15.593	19.701	27.331

after fitting on a particular point a numerical calculation inside the boundary layer with an asymptotic solution outside.

Another comparison can be made with Hinch's asymptotic formulation

$$\alpha \approx 4.0 + \frac{3,219}{\sqrt{Re}} \tag{35}$$

Four experimental results (*Re* = 10, 15, 22.5, 38) (Hinch and Lemaitre (1994) draw attention to the difficulty of measuring the exact distance $\underline{h}$ for a low *Re*) are compared with our numerical results in Figure 9. The error bars on the experimental results were estimated from results given in Hinch and Lemaitre (1994). With a possible experimental measure error of this height, there is an excellent agreement between all the results.

High Re

Our numerical scheme using quasilinearization is able to predict the profiles of the velocity to a Reynolds number greater than 500. Table II gives our numerical results up to *Re* = 550 for the non dimensional wall shear stress on the two surfaces. These results show that the derivative tends asymptotically to a value of 2 as *Re* increases and is approximately equal to the next expression (as soon as the third derivative Z"'(0) is sufficiently small: i.e. *Re* > 15 (Desseaux and Debaillon))

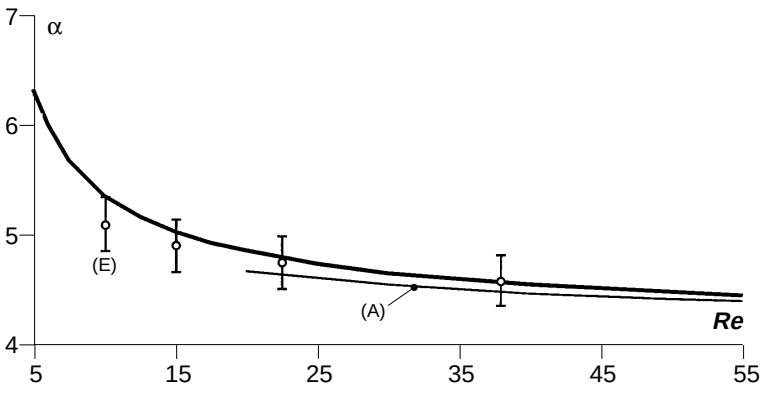

Figure 9. Comparison between our numerical results (full line), experimental values (E) and an asymptotic solution (A) (Hinch and Lemaitre, 1994) for the pressure parameter α

Re	–Z"(0)	Z"(1)	*Re*	–Z"(0)	Z"(1)
100	2.175	38.191	150	2.141	46.507
200	2.121	53.547	250	2.107	59.756
300	2.097	65.373	350	2.090	70.543
400	2.084	75.357	450	2.079	79.882
500	2.074	84.165	550	2.071	88.240

Table II. Numerical solution for high *Re* – the second derivative on both sides

$$-Z''(0) \approx 2. + 2.339\, Re^{-0.558} \tag{36}$$

and the dimensionless wall shear stress on the non-porous disk is approximatively equal to:

$$Z''(1) \approx 4.174\, Re^{0.482} \tag{37}$$

Expressions (35) and (36) inferred by our numerical results are more accurate than an asymptotic development based on the square root of Reynolds number because the determination of the asymptotic solution is limited to the first order of the perturbation parameter.

Figure 10 presents three different illustrations for the vertical velocity. For *Re* greater than 50, the profiles of the vertical velocity are close to each other and this is the reason for not calculating beyond *Re* > 500.

More interesting are the results presented in Figure 11. We can observe the development of the horizontal velocity with the Reynolds number and as the *Re*

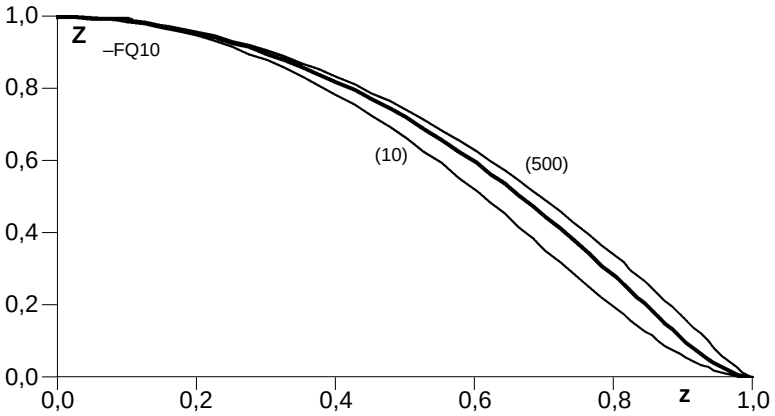

Figure 10.
Comparison for our numerical results between some profiles of the vertical component of the velocity – *Re* = 10; 50; 500

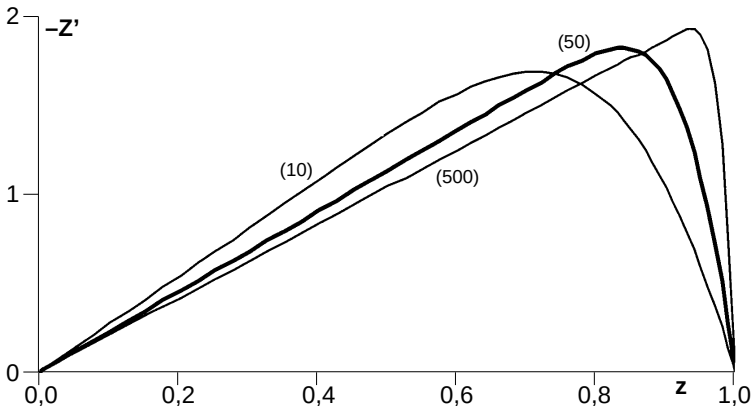

Figure 11.
Comparison for our numerical results between some profiles of the radial component of the velocity – *Re* = 10; 50; 500

grows, we see the reduction of the boundary-layer thickness on the disk. For a *Re* less than 10, the profile of this component is nearly parabolic and can be found using only the lubrification theory (Schlichting, 1968).

Estimation of $\underline{h}$.

The integration of equation (20) using the vertical balance of the forces acting on the disk gives an estimate for the height at which the disk floats, $\underline{h}$ as soon as the mass M of the disk is known:

$$\underline{h} = \frac{\underline{q}.\underline{R}^2}{2}\sqrt{\frac{\alpha\rho\pi}{Mg}} \tag{38}$$

For a practical application of the lift of a disk with any load, it is convenient to use the second evaluation (33) for α. The third derivative of Z on the porous surface is rapidly equal to 0. Then, it becomes, with (35)

$$\underline{h} \approx \sqrt{1. + 1.17\,Re^{-0.558}}\;\underline{q}.\underline{R}^2\sqrt{\frac{\rho\pi}{Mg}} \tag{39}$$

Conclusion

A self-similar solution for the velocity transforms the problem of a disk suspended above a porous surface transformed to a fourth order ordinary non-linear differential equation. Using a quasililearization scheme and replacing the derivatives by five-point central difference approximations, we obtain a system of algebraic equations easy to solve. The numerical results are in very good agreement with those obtained with the use of a general computer program and with experimental results. Our numerical results can predict the height at which a disk floats if we assume that the flow of the fluid across the porous plate is independent of the radial distance under the disk, i.e. that the pressure distribution under the disk is never affected by the geometry.

References

Crnojevic, C., Florent, P. and Decool, F. (1995), "Le champ de pression sur une plaque plane provoqué par un jet d'air", *12e Congrès français de Mécanique*, tome III, Strasbourg, pp. 161-4.

Desseaux, A. and Debaillon, P., "Resolution de l'équation de sustentation pour des nombres de Reynolds", Compris entre 1 et 100, Note interne 950101 – Labde Mécanique des Fluids – Université de Valenciennes.

Gauvain, J., "Bibliographie du programme TRIO-E.F. Logiciel de mécanique des fluides – Développement – Validation – Applications", Laboratoire de Transferts Thermiques et de Mécanique des Fluides, Rapport DMT 94/357, Commissariat à l'Energie Atomique.

Hinch, E.J. and Lemaitre, J. (1994), "The effect of viscosity on the height of disks floating above an air table", *J. Fluid Mech.*, Vol. 273, pp. 313-22.

Magnaud, J.P., Rouzaud, P., Villand, M., Cheissoux, J.L. and Hoffmann, A. (1987), "Recent development in the numerical prediction of thermal hydraulics", *Int. Top Meet. on Adv. in React. Phys; Math. and Comp.*, Paris.

Nakajima, T., Kida, T., Tanaka, T., Morimoto, T. and Yasutomi, Z. (1995), "Numerical simulation on three-dimensional air-cushion and suction pad", *JSME Inter. J.*, series B, Vol. 38 No. 2, pp. 308-17.

Petit, L. (1986), "Sustentation d'un mobile autoporteur sur une table à coussin d'air ou heureusement que l'air est visqueux", *Bulletin de l'union des physiciens*, Vol. 685, pp. 981-91.

Radbill, J.R. (1964), "Application of quasilinearization to boundary layer problems", *AIAA Journal*, Vol. 2 No. 10, pp. 1860-2.

Salvadori, M.G. and Baron, M.L. (1961), *Numerical Methods in Engineering*, Prentice Hall.

Schlichting, H. (1968), *Boundary-Layer Theory*, 6th ed., McGraw-Hill.